GEOPERSIA

Accepted Manuscript

Role of Deep-Rooted Faults in the Generation of Intrashelf Sedimentary Basins in the Central Persian Gulf

Jaber Shoghi, Ahmad Alavi, Iraj Abdollahi Fard, Ehsan Dehyadegari

DOI: 10.22059/geope.2026.413275.648877

Receive Date: 07 May 2026
Revise Date: 12 July 2026
Accept Date: 29 July 2026

Role of Deep-Rooted Faults in the Generation of Intrashelf Sedimentary Basins in the Central Persian Gulf

Jaber Shoghi [1], Ahmad Alavi [1], *, Iraj Abdollahi Fard [2], Ehsan Dehyadegari [1]

[1] Department of Sedimentary Basins and Petroleum Geology, Faculty of Earth Sciences, Shahid Beheshti University, Tehran, Iran
[2] Exploration Directorate, National Iranian Oil Company (NIOC), Tehran, Iran

Received: 07 May 2026, Revised: 12 July 2026, Accepted: 29 July 2026

Abstract
An integrated tectono-stratigraphic approach was applied to investigate the origin and evolution of sedimentary intrashelf basins in the central Persian Gulf (eastern South Pars region). The study combines 2D seismic reflection data, well-log information, subsidence–uplift analysis, and seismic sequence stratigraphy to evaluate the role of deep-seated basement faults in controlling basin architecture and sedimentary evolution. Major deep-rooted fault systems, including the Hamoon, Lavan, Alpha, Sirri, Hendurabi, Razak, Bostaneh and Bastak faults were identified as the principal structural elements governing the development, segmentation, and evolution of the intrashelf basins. The analysis focuses on the Jurassic to Late Cretaceous sedimentary succession, particularly the Surmeh, Dariyan, and Sarvak Formations, using PC-2000 seismic data and well information from the South Pars, Salman, Resalat, Sirri, Kish, Farur, and Reshadat fields. The results demonstrate that differential subsidence and uplift were primarily controlled by the episodic reactivation of deep-rooted basement faults, which generated accommodation space and influenced the spatial distribution of sedimentary depocenters. Salt diapirism locally modified basin geometry and syn-sedimentary topography, whereas eustatic sea-level fluctuations exerted an as well as control on accommodation and facies distribution. The observed tectono-sedimentary evolution is consistent with the progressive reactivation of inherited basement structures during the regional tectonic evolution of the northeastern Arabian passive margin, providing a coherent framework for understanding the development of the Sirri and Hamoon–Balal intrashelf basins. The proposed tectono-stratigraphic model improves the prediction of sediment distribution, reservoir architecture, and hydrocarbon prospectivity, and provides a regional framework for future exploration and tectonic studies in the eastern Persian Gulf.

Keywords: Deep Rooted Faults, Subsidence Analysis, Persian Gulf, Intrashelf Basin.

Introduction

Sedimentary basins form as a consequence of lithospheric subsidence and uplift driven by intraplate and interplate extensional and compressional forces (Allen and Allen, 2013). During continental extension, the lithosphere undergoes thinning, which ultimately leads to the formation of rift systems and associated fault-bounded margins. Depending on their mechanical and thermal evolution, these rifted margins may transition into mature passive margins. Progressive lithospheric thinning and thermal uplift during rifting generate syn-rift subsidence that promotes the accumulation of sediments closely linked to the rift development phase.

The central Persian Gulf—including the South Pars region and its eastern part—offers a unique natural laboratory for investigating the tectonic evolution of an intracontinental rift

* Corresponding author e-mail: J_Shoghi@sbu.ac.ir

system, its transition to a mature passive margin, and its subsequent involvement in orogenic processes leading to foreland basin development (Figure 1). The Persian Gulf Basin, forming the northeastern part of the Arabian Plate foreland system, hosts approximately 40% of the world's hydrocarbon reserves (Bordenave, 2014).

Despite extensive hydrocarbon exploration, the geodynamic history of the Persian Gulf remains inadequately resolved. The primary limitations include the presence of an exceptionally thick sedimentary cover locally exceeding 13 km (Stewart, 2016; Alavi, 2004) and the scarcity of deep seismic imaging and exploratory wells that penetrate the crystalline basement. Consequently, reconstructing the basin's tectonic subsidence and uplift history is essential for understanding the major geodynamic events that shaped the region and for evaluating the role of deep-seated faults in its evolution.

Numerous basement-rooted faults have been reported across the Persian Gulf, fragmenting the underlying crust into distinct structural blocks (Bahroudi and Talbot, 2003; Sepehr and Cosgrove, 2007; Jahani et al., 2017; Mohammadrezaei et al., 2022). This structural segmentation has led to significant variations in the thickness of stratigraphic units throughout the region. Such variations are commonly attributed to differential vertical movements of basement blocks, forming uplifted and depressed domains that influenced the pattern of sediment accommodation. These changes in thickness record multiple tectonic episodes and strongly impact the development of intrashelf basins.

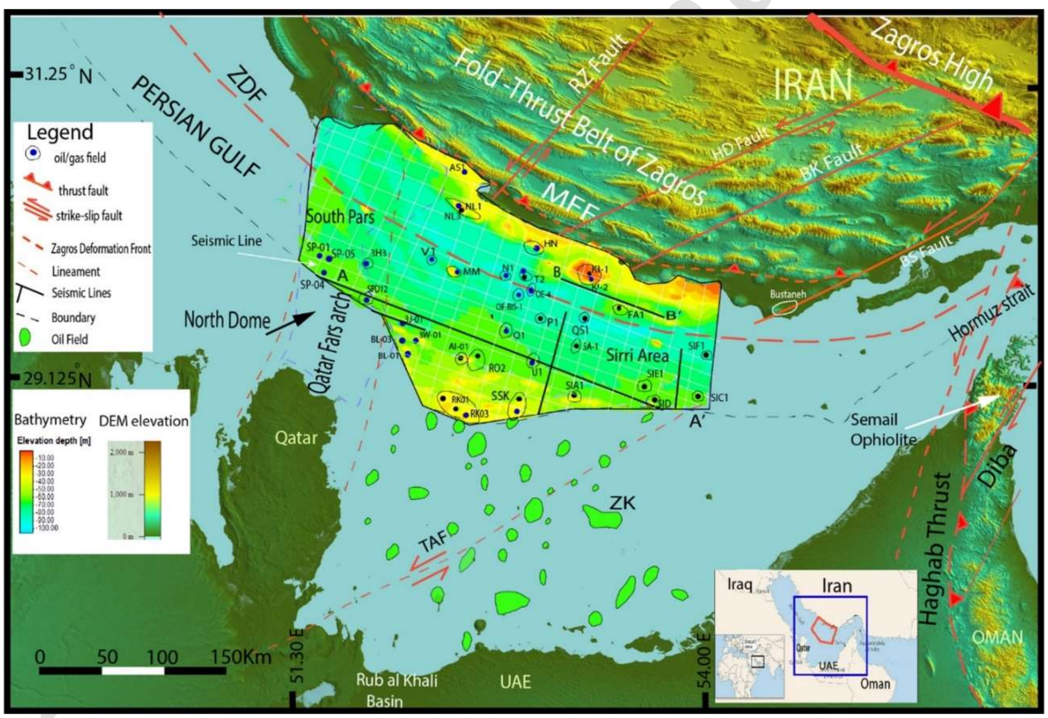

Figure 1. Digital Elevation Map (DEM) with hydrocarbon fields as well as major tectonic structures of the Persian Gulf and Arabian Countries. The study area is indicted in base map with red rectangle (as exploration block A). seismic profiles shown with white colour, yellow seismic lines which have been presented in this study. The fields names: South Pars (SP), Javedan (3J-01), Alpha (Al-01), Rakhsh (RK), Balal (BL), Rostam (RO), Sasan (SSK), Kish (KI), Farur (FA), Hamoon (3H3), Sirri (Sirri's wells), Lavan (NL), Yush (U1), Tondar (T2), Minab (MM), Irish (V1), and Pouria (P1), ZK (Zakum). Other structures/Faults such as: Alvand lineament (AL L.), Lavan Lineament (LA L.), Hamoon Lineament (HA L.), Razak Fault (RZ), Hendorabi Fault (HD), Trans Arabian Fault (TAF), Zagros Deformation Front (ZDF), MFF (Mountain Front Fault), Nezamabad Fault (NZF), Bastak Fault (BKF) and Bostaneh Fault (BSF) are depicted in the figure. The base map image represents a regional paleogeographic reconstruction of the Arabian Plate (modified after Al-Suwaidi and Aziz, 2002)

The resulting cycles of relative sea-level rise and fall produced distinct depositional sequences (Abdollahie Fard et al., 2019; Jahani et al., 2017; Motamedi et al., 2009; Sherkati et al., 2006). Intrashelf basins typically develop within extensive shallow-marine carbonate platforms, where water depths generally range between 50 and 100 meters (Murris, 1980; Vahrenkamp et al., 2010). A period with a worldwide eustatic sea-level highstand (Haq et al., 1987) and a pronounced climatic disturbance recorded by an oceanic anoxic event (OAE).

In this study, we integrate exploratory well data with 2D seismic reflection data from the PC-2000 survey to reconstruct the tectono-stratigraphic history of the central Persian Gulf. Biostratigraphic data from wells covering sedimentary successions from the Permian to the Pleistocene–Holocene were analyzed to evaluate facies variations and paleo-water depths. Using quantitative subsidence analysis through 1D backstripping, we investigate geodynamic processes over the last ~298 million years, including intracontinental rifting, passive margin development, and foreland basin formation. Furthermore, we assess the role of deep-rooted faults and inherited structures in controlling the development of Jurassic and Cretaceous intrashelf basins. Our results reveal a clear correspondence between subsidence trends and the fault activity, demonstrating the fundamental influence of deep-seated tectonics on intrashelf basin formation during the Mesozoic (Bahroudi and Talbot, 2003; Sepehr and Cosgrove, 2007; Sherkati et al., 2006; Mohammadrezaei et al., 2022).

Tectonic Setting

The geological evolution of the Zagros fold-and-thrust belt and the Persian Gulf encompasses principal tectonic phases: Pre-Permian events, Permo-Triassic rifting, Cretaceous to Paleogene subduction, and Neogene continental collision (Berberian and King, 1981; Agard et al., 2005; Sherkati et al., 2006; Jahani et al., 2009; Orang et al., 2018). Although pre-Permian geological information is limited, recent 2D seismic data have provided insights into Hercynian events and potential basement faulting. In the Arabian Shield, basement faults associated with Neoproterozoic to Cambrian structures and the Najd fault system constitute the fundamental framework of the basin. Reactivation of these basement structures has played a pivotal role in shaping the paleogeographic highs and sedimentary basins of the region (Al-Husseini, 2000; Dyer & Husseini, 1991).

Inherited structural trends in the study area exhibit three dominant orientations: North-South, Northwest-Southeast, and Northeast-Southwest (Al-Husseini, 2000; Alavi, 2007). The reactivation of these structures throughout the Phanerozoic has significantly influenced the thickness and distribution of source and reservoir rocks. Seismic evidence indicates that North-South trending basement faults are responsible for normal faulting in Infra-Cambrian units and have played a crucial role in controlling sediment distribution and the evolution of Persian Gulf sedimentary basins (Jahani et al., 2017).

Therefore, analyzing sediment thickness variations from the Permian to the present day offers a clear perspective on the region's tectonic evolution. In particular, studying the stratigraphic changes within the Surmeh, Dariyan, and Sarvak Formations as main intrashelf basins can provide novel insights into the development of intrashelf basins in the area (See Fig. 2).

Data and Methodology

An integrated tectono-stratigraphic workflow was adopted to investigate the structural controls on the development and evolution of intrashelf basins in the central Persian Gulf (eastern South Pars region). The methodology combines geological and geophysical datasets with tectonic subsidence analysis and seismic sequence stratigraphy to evaluate the relationship between basement fault reactivation, differential subsidence, sediment accumulation, and basin evolution.

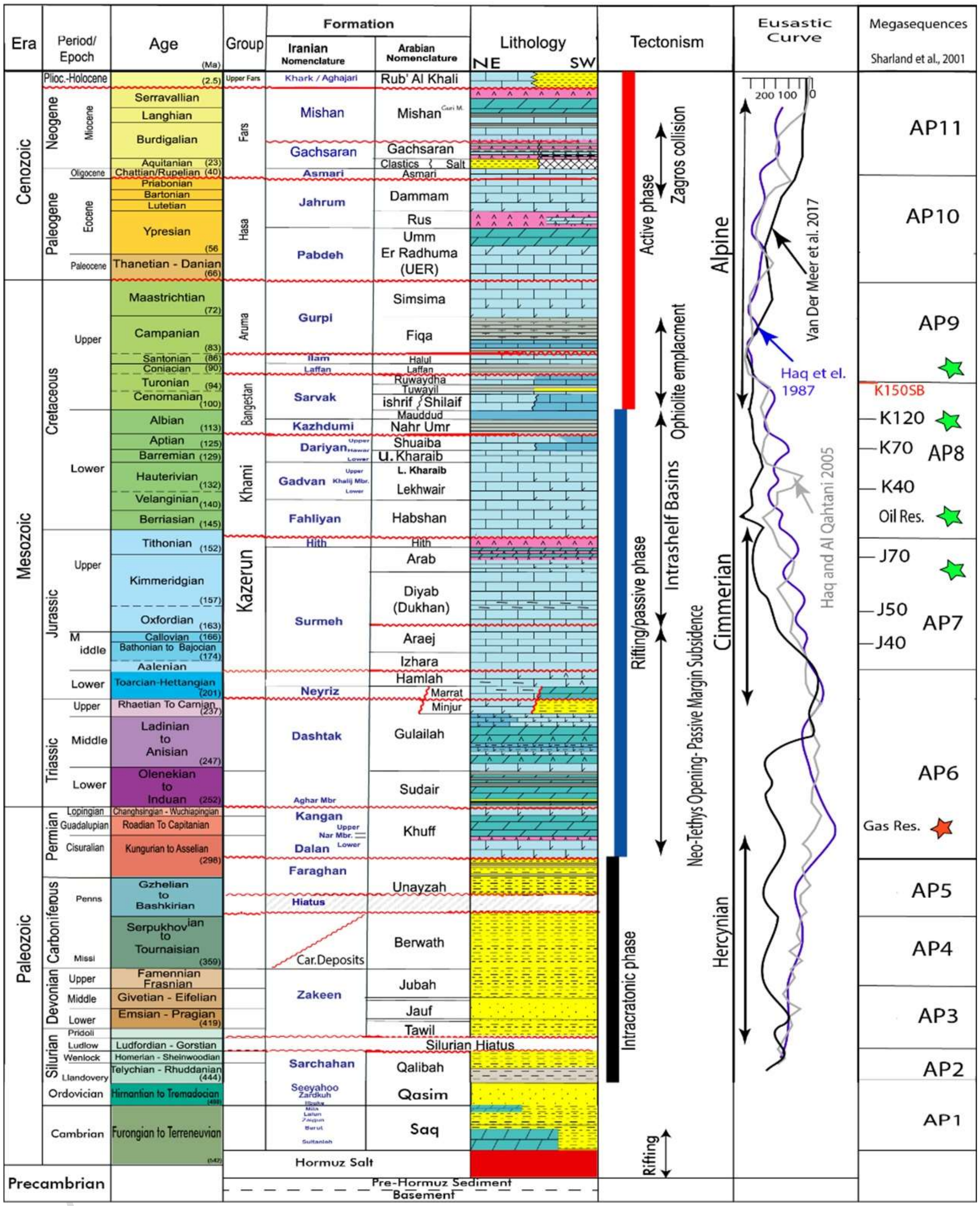

Figure 2. Generalized tectonostratigraphy of Persian Gulf and Arabian Formations (modified after Jabir et al., 2023; Sharland et al., 2001). The geological time scale is adopted from the International Chronostratigraphic Chart of Cohen (2023). Eustatic curves extracted from Haq et al, (1987); Haq and Al-Qahtani (2005) and Van Der Meer et al. (2017), Arabian Plate Tectono-Megasequence boundaries and selected Cretaceous and Jurassic MFS have been extracted from Sharland (2001), Simmons et al. (2007). Red star shows the dominant gas reservoir; the green stars show major oil reservoirs

The database comprises geological and geophysical information from 42 exploration and appraisal wells distributed across the eastern South Pars region. Available well data include lithological descriptions, wireline logs, check-shot surveys, formation tops, and biostratigraphic information, which were used for seismic-to-well calibration, horizon identification, stratigraphic correlation, and age determination. To improve chronostratigraphic constraints in areas with limited age control, regional stratigraphic information from neighbouring wells in the Arabian sector of the Persian Gulf was incorporated using the regional stratigraphic frameworks of Sharland et al. (2001) and Jabir et al. (2023). The principal hydrocarbon fields investigated include South Pars, Balal, Javdan, Hamoon, Tondar, Resalat (Rostam), Rashadat (Rakhsh), Salman (Sasan), Kish, Farur and Sirri.

The seismic database consists of more than 805 post-stack time-migrated two-dimensional (2D) seismic profiles acquired during the PC-2000 survey. Twelve regional seismic horizons, extending from the seabed to the Hercynian unconformity, were interpreted throughout the study area. Particular emphasis was placed on the Jurassic–mid-Cretaceous succession, including the Neyriz, Surmeh, Hith, Fahliyan, Gadvan, Dariyan, Kazhdumi, Sarvak, Gurpi, and Laffan Formations. Seismic interpretation focused on identifying basement faults, structural highs, depocentres, fault geometries, and stratigraphic thickness variations associated with tectonic deformation. Seismic interpretation, structural mapping, well correlation, and isopach map generation were carried out using Petrel® (Schlumberger). Final structural maps and Figs were prepared using Corel DRAW.

Tectonic subsidence was reconstructed using one-dimensional backstripping following the methodology of Sclater and Christie (1980). This technique progressively removes the effects of sediment compaction, sediment loading, water loading, and relative sea-level variations to isolate the tectonic component of basin subsidence. Decompaction was performed using lithology-dependent porosity–depth relationships. Initial porosity and compaction coefficients for each lithology were adopted from Goldhammer (1997), Sclater and Christie (1980) and Schmoker and Halley (1982) are summarized in Table 1.

$$Z = St\,\frac{(pm - ps)}{(pm - pw)} + Wd - \Delta sl\,\frac{pm}{(pm - pw)} \tag{1}$$

In Equation (1), the tectonic subsidence factor (Z) is expressed in metres (m), whereas tectonic subsidence rates discussed in the Results section are reported in metres per million years (m/Ma). The parameters used in the calculation are defined as follows: St, decompacted sediment thickness (m); ρm, mantle density (3300 kg m^{-3}); ρs, average sediment density (kg m^{-3}); ρw, seawater density (1030 kg m^{-3}); Wd, palaeowater depth (m); and ΔSL, relative sea-level variation (m). One-dimensional backstripping calculations were performed using Basin vis, incorporating lithology-dependent decompaction parameters and isostatic corrections.

Palaeowater depths and eustatic sea-level variations were constrained using published regional and global sea-level curves (Haq et al., 1987; Haq and Al-Qahtani, 2005; Van der Meer et al., 2017). Formation ages were determined through lithostratigraphic and biostratigraphic correlations with neighbouring wells and calibrated using the regional Arabian Plate stratigraphic framework (James & Wynd, 1965; Sharland et al., 2001; Jabir et al., 2023).

Table 1. Initial porosity and compaction coefficient used in this study

Lithology	**Compaction coefficient (c)**	**Porosity at the surface (Φ_o)**	**References**
Calcarenites (grainstones)	0.25	0.445	Goldhammer (1997)
Micritic limestones (chalk)	0.71	0.70	Sclater and Christie (1980)
Dolomites	0.216	0.303	Schmoker and Halley (1982)
Limestones	0.52	0.513	Schmoker and Halley (1982)
Pelites (i.e. siltstones and shales)	0.51	0.63	Sclater and Christie (1980)
Sandstones	0.27	0.49	Sclater and Christie (1980)

Subsidence histories reconstructed from the 42 wells were integrated with interpreted seismic sections, structural maps, and depth-converted isopach maps to evaluate the spatial relationship between basement fault reactivation, differential subsidence, uplift, and sediment accumulation. Although one-dimensional backstripping assumes local Airy isostatic compensation and simplifies the three-dimensional geometry of sedimentary basins, the integration of independent geological and geophysical datasets significantly improves the reliability of tectonic interpretations. This integrated workflow provides a robust framework for distinguishing the relative contributions of basement fault reactivation, salt diapirism, and eustatic sea-level fluctuations to the tectono-sedimentary evolution of the Jurassic–Cretaceous intrashelf basins in the eastern South Pars region.

Seismic Interpretation

2D seismic data from the PC2000 survey were utilized for interpreting horizons ranging from the Neogene to pre-Permian strata. Following well-to-seismic calibration, 12 key horizons from the Silurian to the Holocene (including the seabed) were interpreted across the central part of Block A (as Study area). These interpreted horizons, selected based on the sequence stratigraphic framework of the Arabian Plate (Sharland et al., 2001), are as follows: Seabed, Intra-Serravallian (~12 Ma), Intra-Chattian (Upper AP10) (~25 Ma), Pabdeh Formation Top (Upper AP9) (Early Paleocene ~65 Ma), Sarvak Formation Top (Upper AP8) (Mid-Turonian ~92 Ma), Upper Fahlian Formation (Upper Valanginian ~132.9 Ma), Upper Hith Formation (AP7) (Upper Jurassic ~145.5 Ma), Surmeh Formation Top (Upper AP6) (Upper Late Toarcian ~185 Ma), Dashtak Formation Top (Upper Ladinian ~237 Ma), Kangan Formation K1 Top (Upper Olenekian ~247.2 Ma), Upper Dalan Formation Top (Roadian ~289 Ma) (Upper AP5), Faraghan Formation Top (Upper AP4) (Upper Kungurian ~298 Ma), and the Silurian sequence (see Fig. 2 and Fig. 4).

Several dominant normal dip-slip components faults interpreted on the seismic profiles exhibit reflector offsets extending upward through Jurassic units, including associated with Hamoon and Sirri fault systems, which have produced significant subsidence in the eastern South Pars area and the eastern part of the study region. Interpretation of 2D seismic profiles from the central Persian Gulf (CPG) region, integrated with published structural studies (e.g., Bahroudi and Talbot, 2006; Sherkati et al., 2006; Jahani et al., 2017), demonstrates that most mapped faults (see Fig. 3) and lineaments within the Zagros Fold–Thrust Belt are basement faults. Instead, deformation is predominantly confined to the sedimentary cover and is mechanically decoupled above the Hormuz salt unit, which acts as the main regional décollement.

Although the Hamoon and Sirri faults exhibit apparent vertical continuity within the supra-salt sedimentary succession, their seismic expression becomes obscured within the Hormuz Salt due to the highly ductile rheological behavior and poor seismic imaging characteristics of the evaporitic sequence. Consequently, fault traces cannot be reliably followed through the salt interval. Whereas, beneath the Hormuz Salt, deep-seated fault segments reappear within the pre-salt succession, suggesting that these structures continue at depth despite the loss of seismic continuity across the salt layer. However, they cannot be traced through the salt layer, and their geometry is strongly influenced by prominent salt diapirs that generate sharp structural boundaries, and isolated intra-basinal domains and Carbonate platform (Fig. 5). In other hand, the three-dimensional gravity inversion study conducted by Eshaghzadeh et al. (2014) provides valuable insights into the basement configuration and sedimentary architecture of the Persian Gulf Basin. As illustrated in Fig. 3b, positive gravity anomalies correspond to basement uplifts, whereas negative anomalies delineate basement depressions associated with thicker sedimentary accumulations. The map also highlights the locations of the major regional faults.

The inversion results indicate sediment thicknesses of up to approximately 13 km above the crystalline basement and reveal a highly heterogeneous basement relief, reflecting the complex tectonic history of the study area. Overall, the interpreted gravity model demonstrates that basement faulting has exerted a primary control on the structural framework of the basin and the spatial distribution of sedimentary sequences, consistent with the findings of Eshaghzadeh et al. (2014).

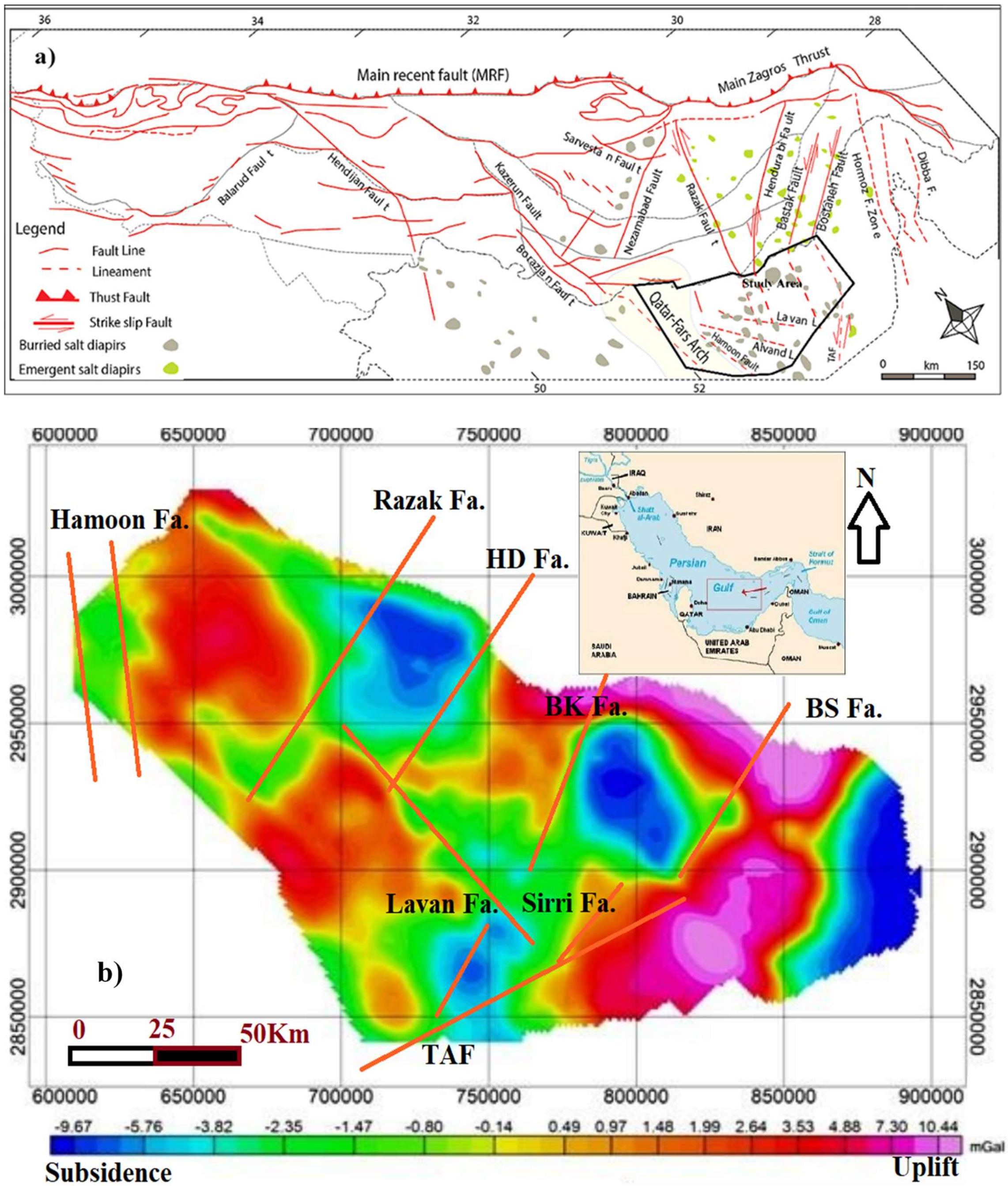

Figure 3. a) Main faults and lineaments in Zagros and Persian Gulf along with salt distribution (Modified after Jahani et al., 2009; Bahroudi and Talbot, 2006 and Sherkati et al., 2006). b) Residual Gravity Anomaly of basement Map of the exploratory region in study area (modified after Eshaghzadeh et al., 2014)

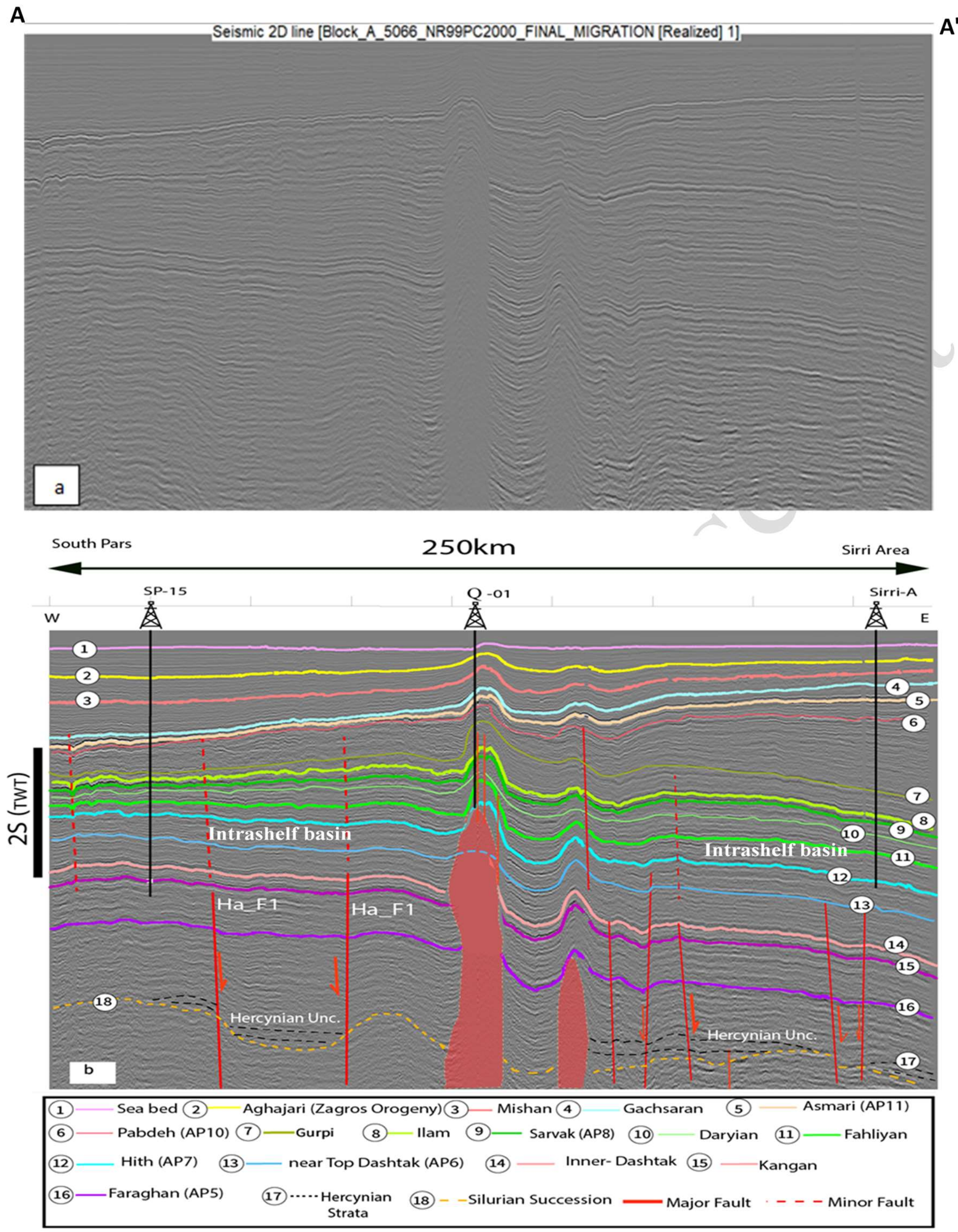

Figure 4. a) Uninterpreted 2D seismic line (A-A'), b) Same seismic line from study area No:5066, which includes the interpretation from the seabed to the Silurian, along with salt diapirs showing deep faults moving toward younger layers. Hamoon (Ha) deep faults which cut through the Silurian to Permian units have resulted in forming deep basins in the surrounding areas of these faults and salts. Fig. 1 displays the location of the seismic line

2D seismic data from the study area demonstrate the regional Hercynian unconformity, which consistent with Faqira et al. (2009) and Konert et al. (2001) reports, this unconformity is characterized by erosional truncation and pronounced paleotopographic relief resulting from Late Paleozoic tectonic deformation and erosion (see Fig. 4). This structural configuration closely resembles that observed in the Arabian sector of the Persian Gulf.

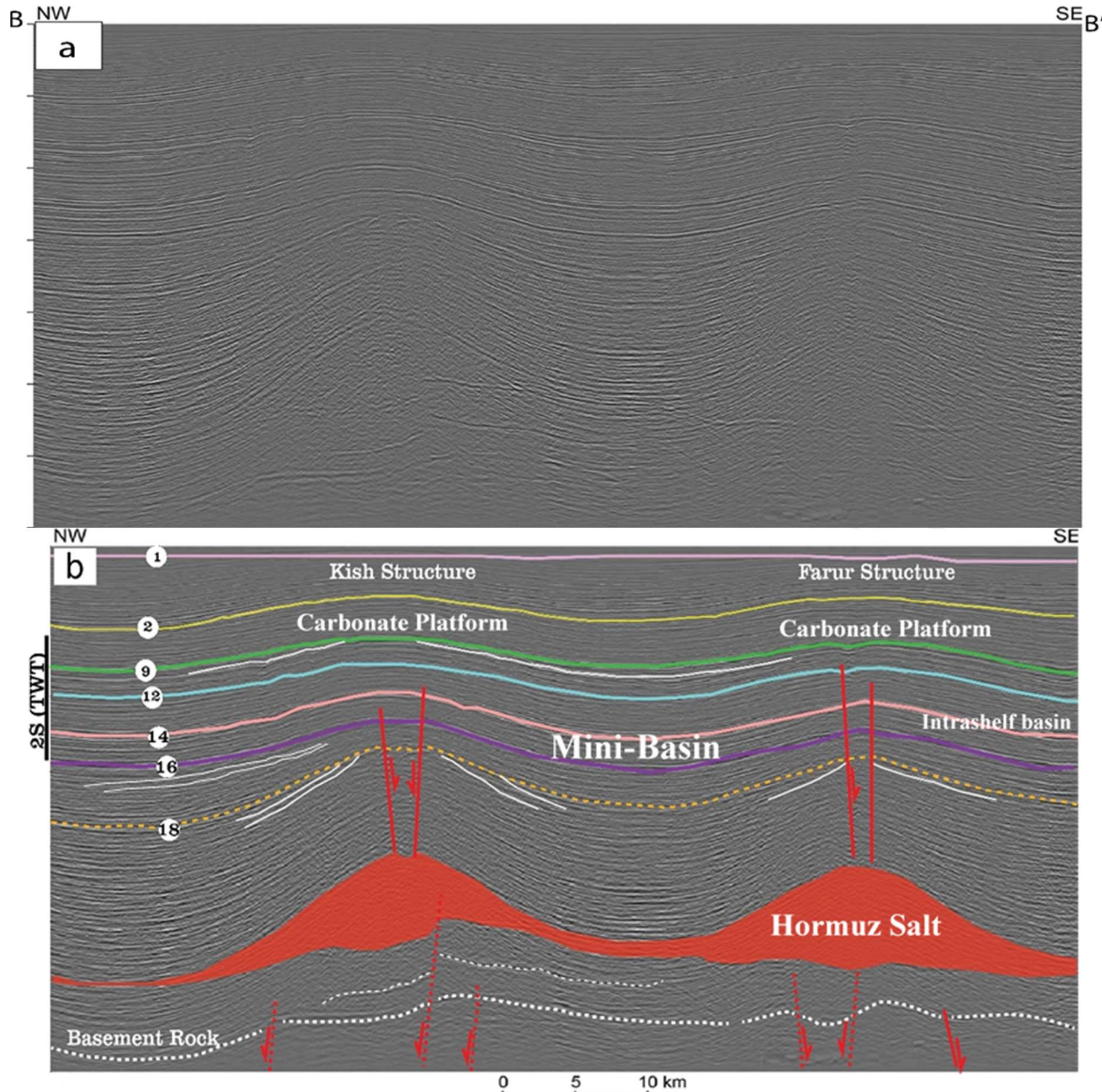

Figure 5. a) Uninterpreted 2D seismic line (B-B'), b) Seismic interpretation-oriented NW-SE over the two significant structures of Kish and Farur. It shows the role of basement faults in forming sub-Permian salt basins and mini-basins around the structures created due to salt movement. The deep normal fault is located at a depth of about 13 km, approximately below salt layers. Some horizons are not intentionally shown due to focusing the basement interpretation. Figure 1 show the position of the seismic lines. Horizons legend as well as those code is depicted in Figure 4

Results

Sedimentation History

The Permian–Neogene stratigraphic succession of the Persian Gulf records the development of intracontinental basins and the widespread deposition of shallow-marine carbonate sediments across the Arabian continental shelf. This study investigates the distribution of intrashelf basins within the Surmeh, Dariyan, and Sarvak Formations. These formations correlate regionally with the Jurassic Arab, Diyab, Araej, and Izhara formations (Wilson, 2020d), the Aptian Shuiba–Bab succession (van Buchem et al., 2010), and the Cenomanian–Turonian Mishrif–Shilaif Formation (Bromhead et al., 2022) across the Arabian Plate.

The stratigraphic framework was established using well-log and lithostratigraphic data from the study area, while chronostratigraphic ages were adopted from Sharland et al. (2001), Davies et al. (2002), and Simmons et al. (2025). Fig. 6 presents a stratigraphic correlation panel flattened at the top of the Sarvak Formation, highlighting lateral variations in formation thickness and lithofacies architecture. The correlation panel illustrates the spatial distribution and facies variability of the Surmeh, Dariyan, and Sarvak Formations across the study area.

Correlation of wells from the South Pars, Javdan, Rakhsh, Salman, Yoush (U1), and Sirri fields (see Fig. 6) reveals a systematic eastward increase in formation thickness accompanied by a gradual transition toward deeper-water carbonate facies. This stratigraphic trend is interpreted to reflect deposition within an outer-ramp to intrashelf basin setting, indicating progressive deepening of the depositional environment toward the eastern part of the study area. Fig. 6 further illustrates major tectonic events, identified as sequence boundaries, in conjunction with thick sedimentary–tectonic sequences and maximum flooding surfaces pertinent to the Jurassic and Cretaceous periods, depicted within selected stratigraphic columns. Gross depositional facies were interpreted through the analysis of biozones and available core data, revealing transitions from shallow-marine carbonates and organic-rich carbonates to evaporites and fine-grained clastic units. Crucially, key petroleum system elements—including source rocks (SR), carbonate reservoirs (R), and sealing facies (S)—have been identified within this framework.

The Sarvak Formation, as presented in Fig. 6, exemplifies east-west facies transitions, progressing from platform settings to intrashelf basin environments, accompanied by significant thickness variability. The Mauddud Member, however, demonstrates remarkable lateral continuity, indicative of regionally stable depositional conditions. In contrast, the oligosteginid-rich marly–shaly interval (equivalent to the Ahmadi/Shilaif Formations) in Sirri area (Mehrabi et al., 2015). In contrast significant thinning over structural highs, such as the South Pars structure. This thinning points to reduced accommodation space and sediment bypass during its deposition. Within the Sirri wells, facies rich in calcispheres are observed to coincide with highstand systems tracts, reflecting periods of diminished carbonate productivity. Furthermore, the South Pars area experienced a Turonian-aged uplift and erosion event, which clearly defines the K150 sequence boundary (K150SB). Notably, thickness variations in the eastern sector, particularly evident in the Javadan well, are strongly influenced by the Hamoon fault.

The Dariyan Formation is subdivided into three distinct units, following the classical model (e.g., van Buchem et al., 2010), as visually represented in the correlation panel (Fig. 6). The Lower Dariyan (Kharaib equivalent) is characterized by shallow, dense platform carbonates. The Middle Dariyan (Hawar Member) comprises marls and calcareous mudstones, indicative of a facies shift towards deeper-water conditions across the Arabian Plate. The Upper Dariyan (Shu'aiba equivalent) displays considerable lateral facies variability, predominantly featuring Orbitolina-bearing carbonates. This unit transitions eastward into clay-rich basinal facies within the Bab Basin domain, as observed in the Sirri and Farur area. The Surmeh Formation comprises four distinct lithological units observed in the Salman, Rakhsh and Rostam fields . Based on graphic well logs from the fields, the studied Jurassic succession is subdivided into four main parts. The lower part consists of light to dark grey limestone and green shale, interbedded with thin layers of argillaceous limestone containing *Lithiotis* fossils. The middle part is characterized by alternating beds of dolomite, argillaceous lime mudstones, bioclastic–peloidal packstones, oolitic grainstones, as well as intraclastic wackestones and packstones. The third part comprises lime mudstone to wackestone and packstone, calcareous shales, and oolitic packstone–grainstone, which is considered equivalent to the Diyab Formation. Overlying this interval, the fourth uppermost unit of the Surmeh Formation, known as the Arab Member, consists of cyclic alternations of limestone, dolomite, and anhydrite, correlative with the Arab Formation.

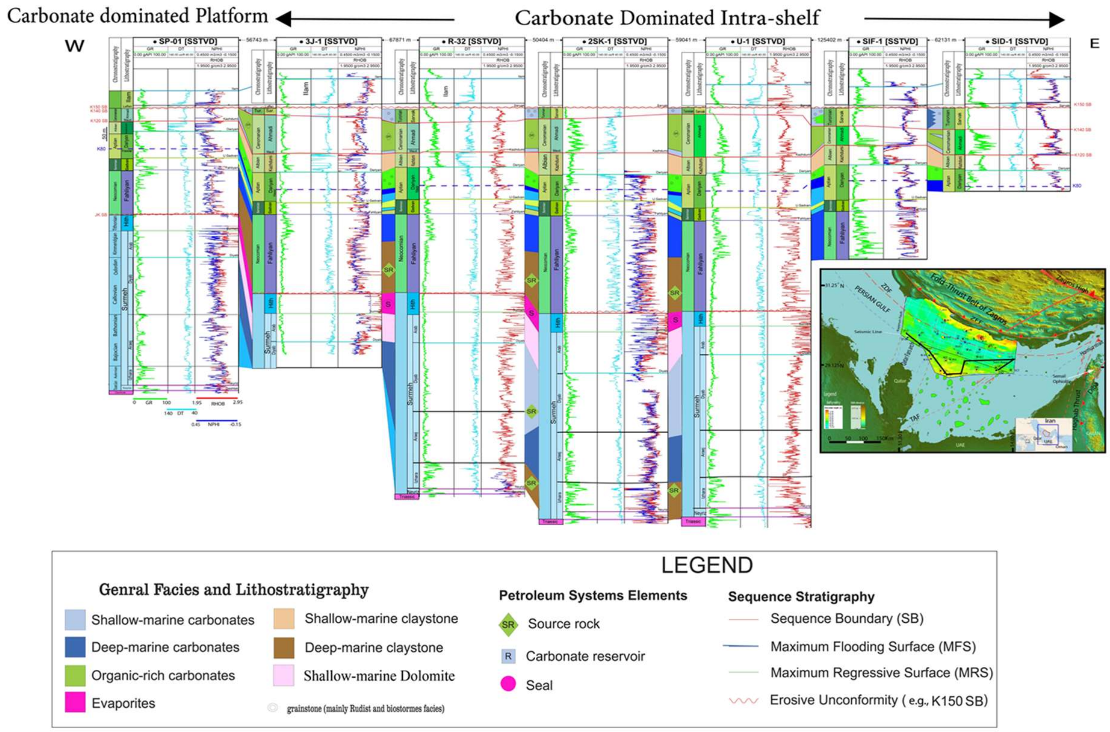

Figure 6. Well correlation from west to east, Sarvak Formation is Flattened. Electrical logs containing gamma, sonic, density, and neutron data from the exploratory-production study area wells include South Pars (SP1), Javedan (3J-01), Rakhsh (RK-02), Sasan (2SKD), Yush (U-01), Sirri F, and Sirri D, representing the thickness and facies changes in the Sarvak, Dariyan, and Surmeh Formations, base map show location of well section. Applying the sequence stratigraphic boundary and Maximum Flooding Surface scheme of Sharland et al. (2001) and Simmons et al. (2025)

1D Backstripping

Analysis of subsidence and uplift based on the burial-time plot using the backstripping Eq-1 was conducted for 42 wells in the study area. Fig .7 shows representative well of SP-01 illustrate an initial increase in subsidence around 270 million years ago during the Permian, coinciding with the deposition of the Dalan Formation over the Faraghan Formation. This phenomenon indicates a marine transgression over Faraghan clastic sediment (see also Figs. 7 and 8).

Subsequent to this phase, a passive basin with subsidence rates of 10 to 20 meters per million years ensued until the Early Jurassic. The second phase of sudden subsidence increase is observed in the Middle Jurassic, attributed to the expansion of the Neotethys basin. The burial plot demonstrates subsidence rates of 80 meters per million years during the Permian and 100 meters per million years during the Middle Jurassic. Thereafter, sedimentation in a post-rift environment due to extensional tectonics from the Middle Jurassic to the Cenomanian affected sedimentation dynamics and led to the development of intrashelf basins between uplifted regions associated with pre-existing structures and those resulting from the upward movement of salt series such as Hormuz (Murris, 1980; Wilson, 2020d).

Total 42 wells subsidence history is shown in Fig. 8 for time span180 Ma. This burial history not only illustrates subsidence but also highlights the uplift processes resulting from the reactivation of inherited structures. Notable tectonic uplift events were observed during four distinct time intervals: Late Triassic to Early Jurassic, Late Jurassic to Early Cretaceous, Cenomanian to Turonian, and Oligocene to Miocene (see Fig. 8). The analysis of subsidence history and seismic data in the South Pars region reveals significant uplift beginning from the Late Jurassic to Early Cretaceous.

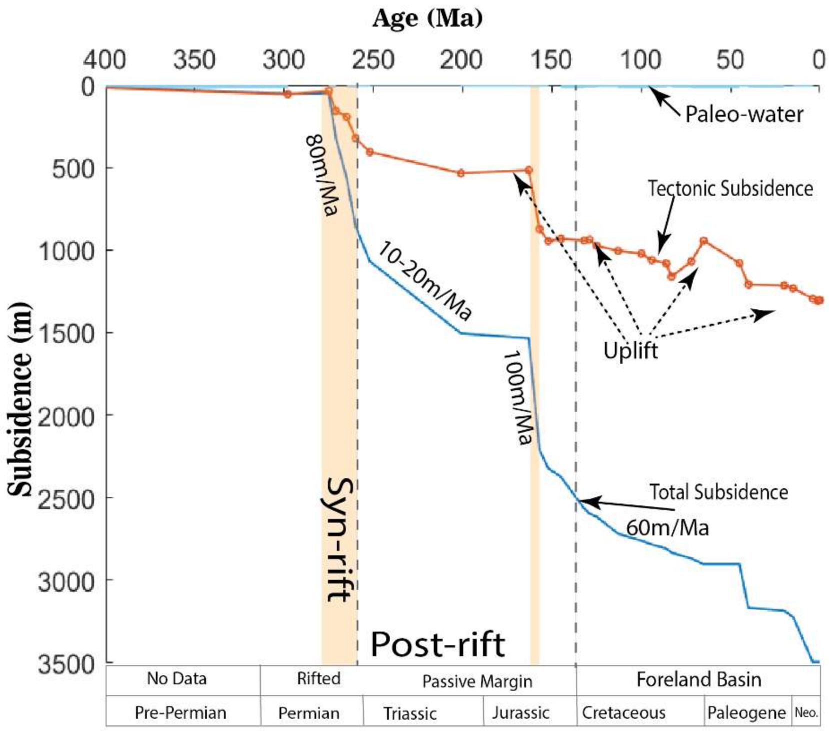

Figure 7. Tectonic and Total subsidence curves obtained for the sedimentary successions of the Central Persian Gulf Basin (SP1). In this diagram, two stages of sharp subsidence are observed, with the first stage associated with rifting and the formation of the Neo-Tethys, and the second stage related to the basin's relaxation phase, indicating post-rift conditions in the region. The sequences corresponding to the syn-rift, post-rift, and foreland are also clearly visible. Four uplift events are recognized. Subsidence rates in the four time intervals are depicted in picture (Modified after Shoghi et al., 2025)

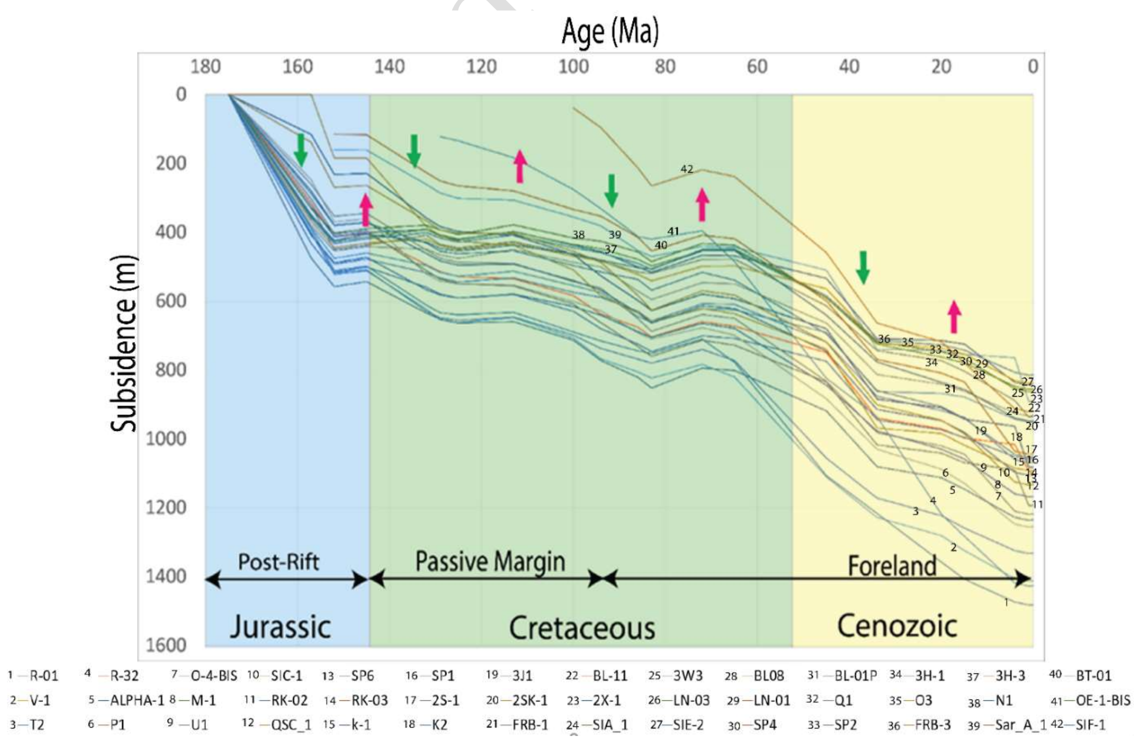

Figure 8. Tectonic subsidence vs time curve showing for 42 wells for time span 180 Ma, derived from well data. The curve illustrates uplift and subsidence events (green: Subsidence and red: Uplift)

Thickness variations

Isopach maps derived from subsurface underground maps provide essential insight into the tectonic controls and mechanisms governing the evolution of intrashelf basins. By illustrating spatial variations in sediment thickness, these maps clarify depositional patterns within the Jurassic, Aptian, and Cenomanian–Turonian successions.

The isopach map of the Surmeh Formation (Fig. 9a) correlative with the Arab, Diyab, Uwanat, Araej, and Izhara units shows a pronounced thinning over the South Pars paleohigh. In contrast, substantial thickening occurs across structures such as Sasan, Rakhsh (Reshadat), Rostam (Resalat), and Farur. Enhanced sediment accumulation is particularly evident in the southern and eastern parts of the study area, including the Sasan, Rakhsh, and Rostam fields, as well as the Sirri E and F area. Thickness variations shows closely to major structural trends, especially the dominant north–south (N–S) and northeast–southwest (NE–SW) oriented systems associated with the Sirri, Hamoon, Lavan, Alvand, and Razak faults.

In Rostam field and the areas surrounding the Sasan field, Surmeh thickness reaches up to 660 m, whereas in South Pars it decreases to about 440 m. This contrast highlights the significant influence of pre-existing structural uplifts on the thickness architecture of the formation.

The isopach map of the Dariyan Formation indicates an average thickness of approximately 90 m in South Pars, with an overall N–S trend. The eastern margin of this structure exhibits thickening, while several fields display localized thinning anomalies. The central part of the region is affected by the Razak and Hendurabi fault systems. In the eastern portion of the study area—particularly toward the Farur block—Dariyan thickness reaches up to 190 m. Conversely, the southeastern sector, including the Sirri area, shows evidence of uplift attributed to salt movement (Fig. 9b).

The Sarvak Formation isopach map reveals significant thinning during the Cenomanian–Turonian interval in the western part of the study area, in eastern South Pars. In contrast, marked uplift across South Pars during this time led to erosion or complete non-deposition of large portions of the original Sarvak sequence. The dominant N–S thickness trends observed region showing the controlling role of inherited basement structures and salt-related tectonics (Fig. 9c). Upward salt migration is evident in the Kish, Rostam, and Hamoon fields, whereas basement fault reactivation produced substantial uplift across the South Pars region. In certain areas, such as Farur, considerable Sarvak thickening is observed along a N–S trend, likely related to the influence of the Sirri structural system and, farther landward, the Bastak and Bostaneh fault zones.

A regional structural cross-section extending from the South Pars field to the Sirri field was constructed to illustrate the principal structural features associated with lateral variations in sedimentary thickness across the study area (Fig. 10). The cross-section displays the interpreted stratigraphic horizons from sea level to the inferred crystalline basement, together with the locations of the major regional faults and the Hormuz Salt.

The cross-section shows pronounced lateral variations in the thickness and geometry of the sedimentary succession. Changes in stratigraphic thickness are spatially associated with deep-seated basement faults, while deformation of the overlying sedimentary units is observed in areas affected by Hormuz Salt structures. These structural elements can be traced throughout the section from the seafloor to the interpreted basement, highlighting the structural complexity of the study area. At the regional scale, these vertical movements are interpreted to reflect the long-term tectonic evolution of the northeastern Arabian Plate. During the Mesozoic, the study area formed part of a broad passive continental margin along the southern Neo-Tethys Ocean, where thermal subsidence provided the regional accommodation space for extensive carbonate deposition. Superimposed on this long-wavelength subsidence, episodic reactivation of inherited Precambrian basement faults generated localized uplift and subsidence, leading to the development of structural highs, depocenters, and intrashelf basins.

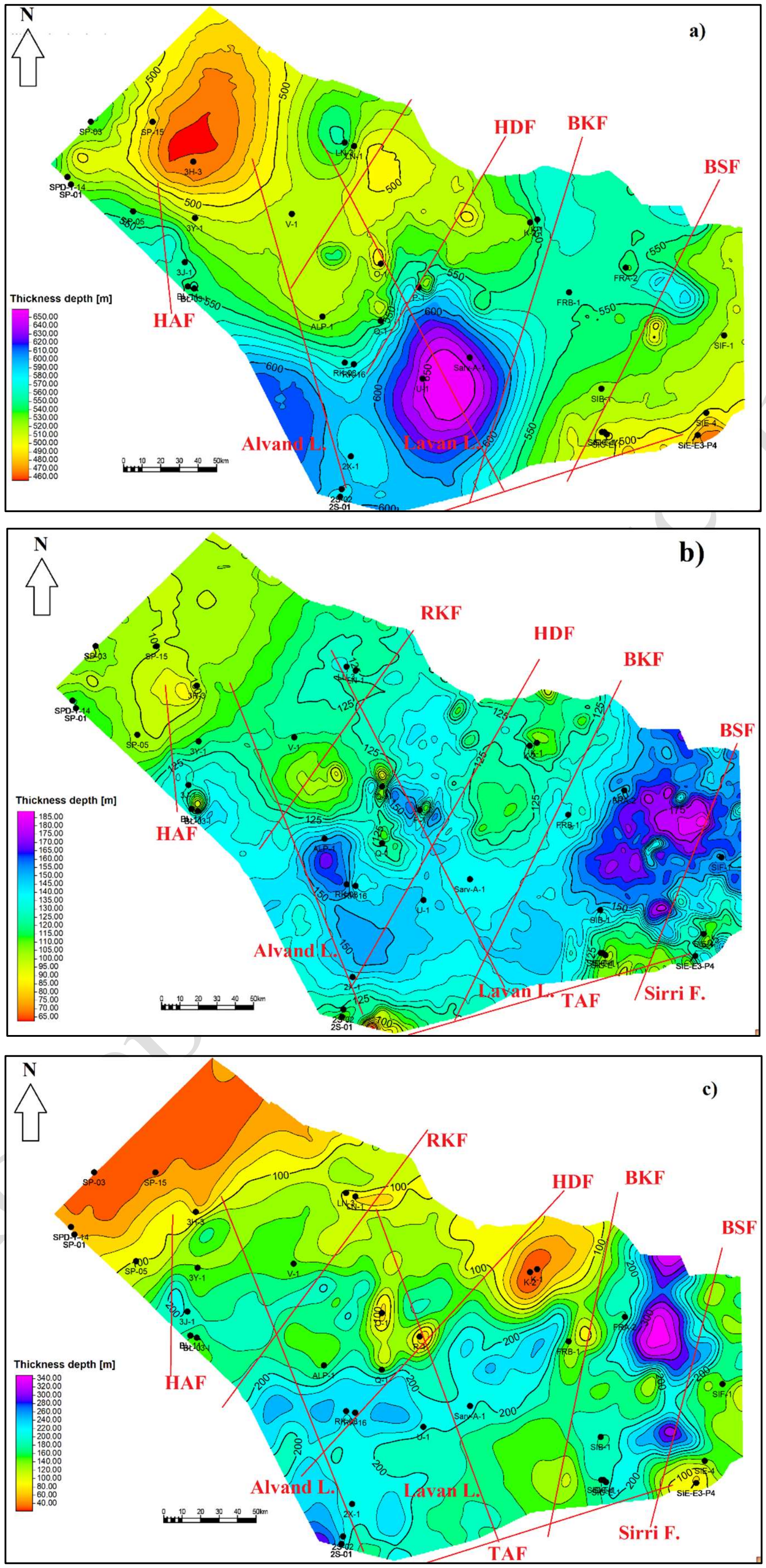

Figure 9. a) Isopach map of the Surmeh Formation, b) Isopach map of the Dariyan Formation, c) Isopach map of the Sarvak Formation

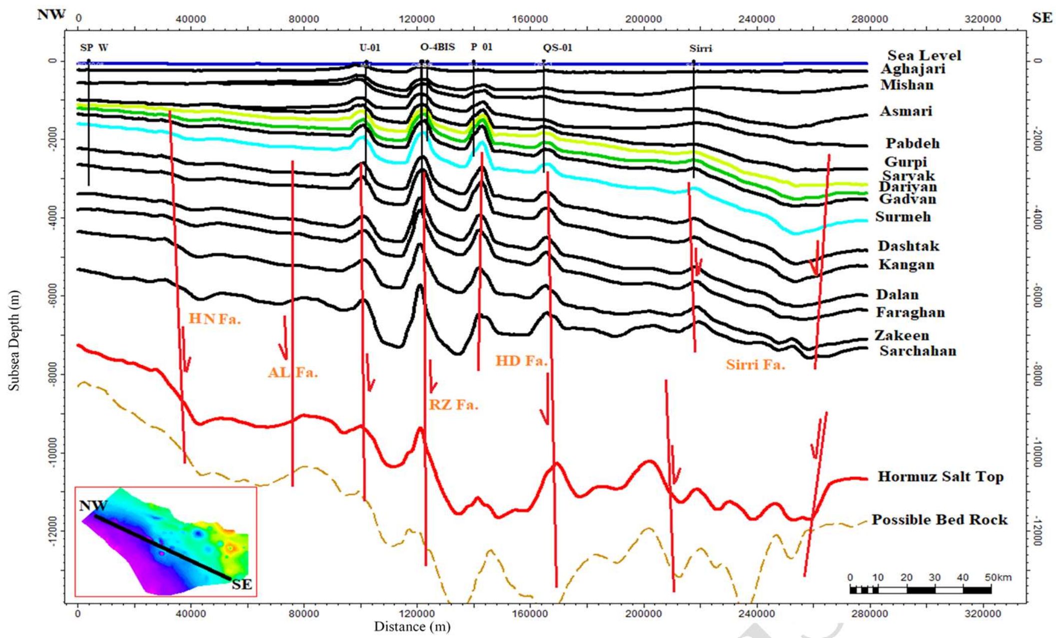

Figure 10. Regional structural cross-section from the South Pars to the Sirri area showing the interpreted stratigraphic horizons, major basement faults, Hormuz Salt, and sediment thickness variations

The onset of convergence between the Afro-Arabian Plate and Central Iran, associated with the progressive closure of the Neo-Tethys during the Late Cretaceous and Cenozoic, likely enhanced the reactivation of these inherited basement structures. Rather than creating the original basin geometry, this convergence amplified pre-existing structural relief through differential vertical displacement of basement blocks, thereby modifying sediment accommodation and influencing the distribution and preservation of carbonate successions.

Within the regional paleogeographic framework, the study area occupied the northeastern margin of the Arabian Plate and evolved as part of a shallow carbonate platform punctuated by periodically developed intrashelf basins. The spatial distribution of thicker successions in the eastern part of the study area is consistent with published paleogeographic reconstructions, which indicate progressive deepening toward the Neo-Tethyan basin and the establishment of outer-ramp to intrashelf basin depositional environments during the Jurassic to Cretaceous.

Tectonic Subsidence

Cenomanian (ca. 92 Ma)

The subsidence map for the Cenomanian (Fig. 10a) reveals pronounced tectonic subsidence ranging from ~200 m to ~1700 m, following a dominant north–south trend in the eastern Persian Gulf. This period coincides with intensified halokinetic activity, which contributed to the development of foreland basins (Fig. 11a).

Well data indicate significant temporal and spatial variability in subsidence rates. Differential subsidence and localized uplift played a critical role in salt mobilization through differential loading, a key mechanism in salt tectonics. Major structural lineaments—including the Hamoon, Alvand, Lavan, Sirri, RK, and HD trends exerted a structural control on Sarvak Formation subsidence, predominantly through normal fault displacement.

Facies analysis from well logs demonstrates that areas of maximum subsidence are characterized by deposition of deeper marine facies, indicating that tectonically driven accommodation space strongly influenced depositional environments and lateral facies variability.

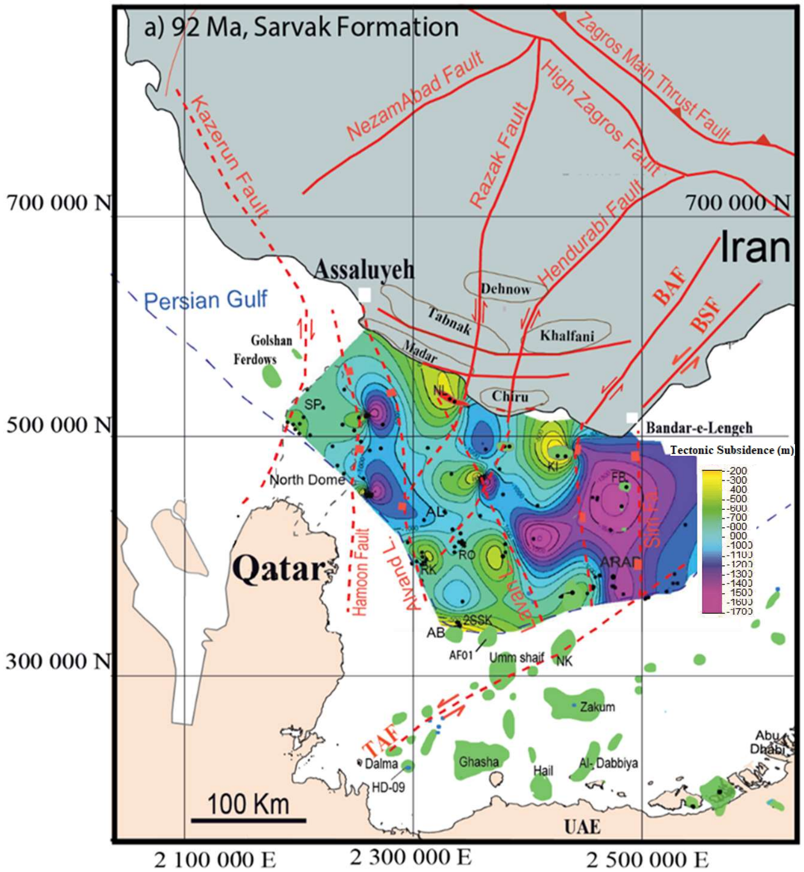
a) 92 Ma, Sarvak Formation
Zagros Main Thrust Fault
NezamAbad Fault
High Zagros Fault
Razak Fault
Kazerun Fault
Hendurabi Fault
700 000 N
700 000 N
Iran
Assaluyeh
Persian Gulf
Dehnow
Tabnak
Khalfani
BAF
BSF
Golshan
Ferdows
Madar
Chiru
Bandar-e-Lengeh
500 000 N
Tectonic Subsidence (m)
North Dome
Qatar
Hamoon Fault
Alvand L.
Lavan L.
Sirri Fa.
300 000 N
Umm shaif
Zakum
TAF
Dalma
HD-09
Ghasha
Hail
Al- Dabbiya
Abu Dhabi
100 Km
UAE
2 100 000 E
2 300 000 E
2 500 000 E

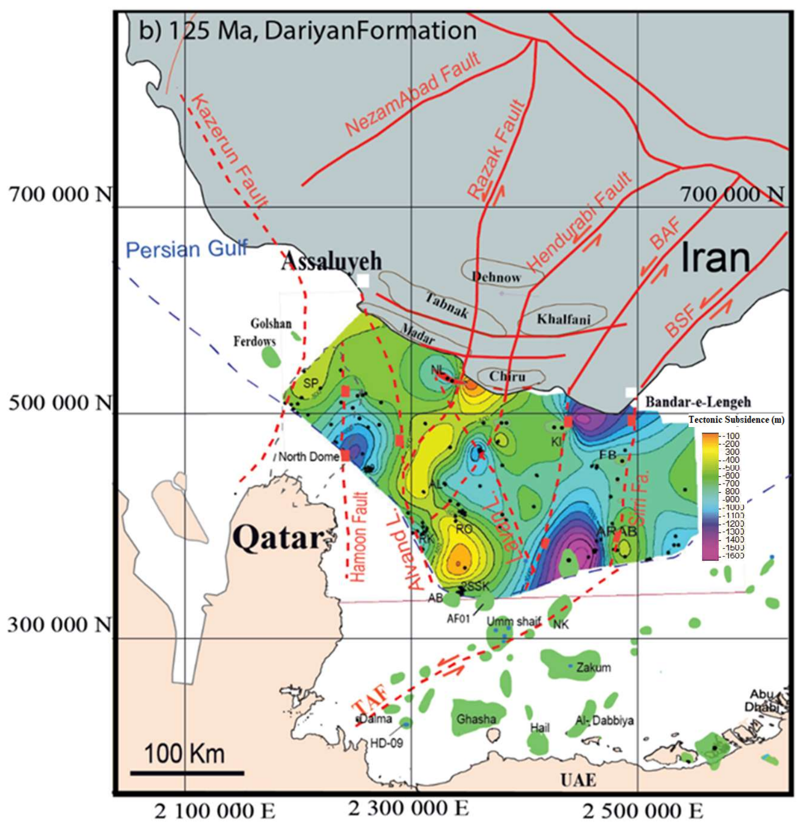
b) 125 Ma, DariyanFormation
NezamAbad Fault
Kazerun Fault
Razak Fault
700 000 N
700 000 N
Hendurabi Fault
BAF
Iran
Persian Gulf
Assaluyeh
Dehnow
Tabnak
Khalfani
BSF
Golshan
Ferdows
Madar
Chiru
Bandar-e-Lengeh
500 000 N
Tectonic Subsidence (m)
North Dome
Qatar
Hamoon Fault
Alvand L.
Lavan L.
Sirri Fa.
300 000 N
Umm shaif
Zakum
TAF
Dalma
HD-09
Ghasha
Hail
Al- Dabbiya
Abu Dhabi
100 Km
UAE
2 100 000 E
2 300 000 E
2 500 000 E

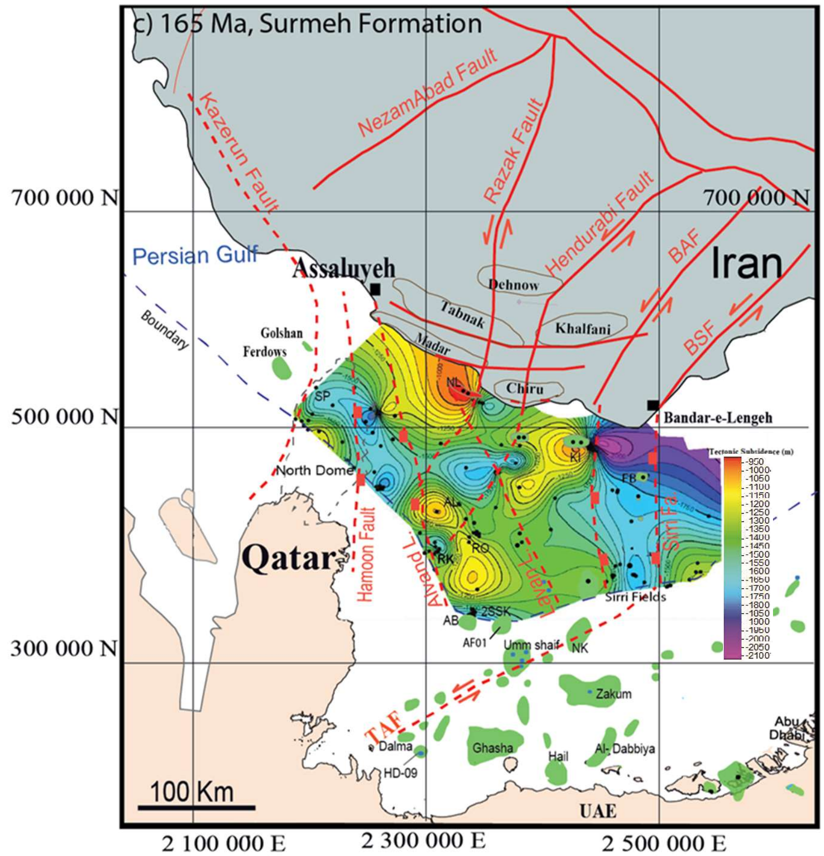

Figure 11. a) Subsidence and uplift map of the Sarvak Formation (Cenomanian ~ 92 Ma), b) Subsidence and uplift map of the Dariyan Formation (Aptian ~ 125 Ma), c) Subsidence and uplift map of the Surmeh Formation (Bathonian ~ 175 Ma)

Aptian (ca. 125 Ma)

The Aptian subsidence map shows a major depocenter east of the South Pars area, with a north–south-trending zone of enhanced subsidence extending from Lavan southward toward the Reshadat structure. The overall geometry is comparable to the Cenomanian pattern, suggesting structural inheritance. In the Sirri area, tectonic subsidence exceeds 1600 m, marking it as one of the principal depocenters during this interval. These findings indicate persistent structural control on accommodation development from the Early to Late Cretaceous (Fig. 11b).

Middle Jurassic (ca. 165 Ma)

The tectonic subsidence map for approximately 165 Ma (Fig. 11c), corresponding to deposition of the Middle Surmeh Formation (equivalent to the Diyab Formation in the Arabian Plate), indicates subsidence exceeding 2700 m during the Middle Jurassic. Structural trends observed in this interval align with major north–south-oriented lineaments such as Razak, Sirri, Lavan, and Alvand, as interpreted from 2D seismic data.
Subsidence patterns during the Callovian–Oxfordian exhibit both north–south and northwest–southeast orientations, reflecting the influence of regional structural fabrics. The deposition of the Surmeh Formation (correlative with the Arab, Diyab, and Izhara Formations) occurred under intracontinental basin conditions characterized by substantial tectonic subsidence and structural compartmentalization.

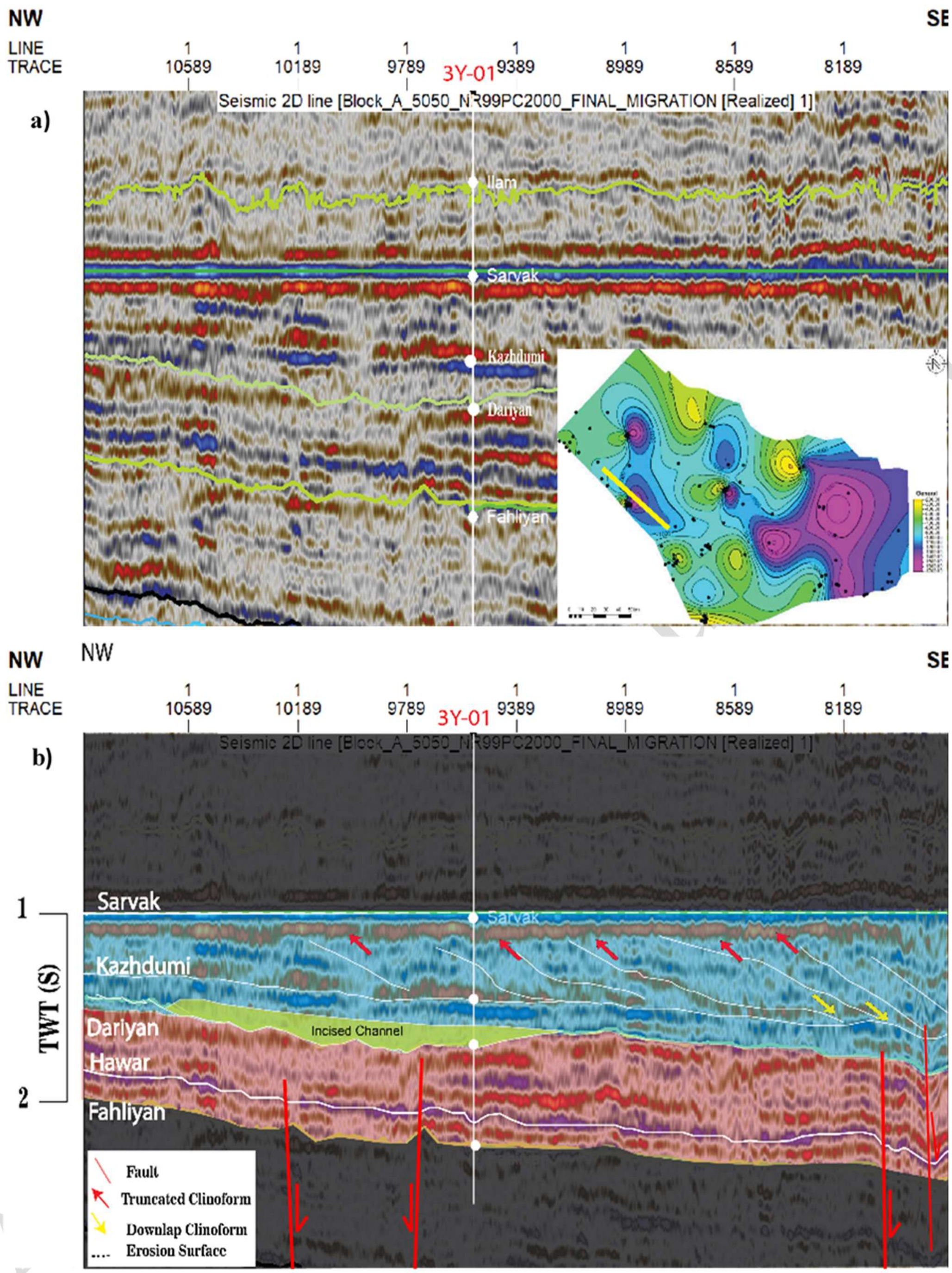

Figure 12. a) Seismic line 5050 shows major horizons interpretation on Yalda structure, horizon flattened on Sarvak (3Y-01 well) : Base map is subsidence map b) 2D seismic profile with interpretation of the Intrashelf basin location, along with the Clinoforms sedimentation geometry in the eastern part of the South Pars area within the Sarvak formation; Base map is Total subsidence map

Seismic Stratigraphy validation

Seismic stratigraphy, as a branch of geophysics, uses seismic reflectors and sequence patterns to investigate the depositional evolution and the development of sedimentary environments at the intra formational scale (Vail et al., 1987). Seismic and well cross-sections indicate that these basins were influenced by deep-seated fault activity and salt movement, leading to localized subsidence or differential uplift. By analyzing the geometry of seismic reflections, this method allows the identification of changes in sea level during deposition and the recognition of faults activity.

In the seismic data, the geometries of oblique reflectors were identified as progressive clinoforms (progradational geometries). Seismic line 5050 is interpreted in the Sarvak Formation shows clinoforms sigmoidal shape, prograding eastward from the South Pars area towards the Yalda Field (3Y-01) (see Fig.12). Distinct horizontal reflectors are observed over the carbonate platform, while seismic reflections associated with grainstone facies are concentrated near structural crests. Conversely, reflections linked to finer-grained facies are observed along the flanks, transitioning towards the intrashelf basin. Interpreted faults correspond to Hamoon fault system which effect on the basin slop. A prominent incised channel feature is interpreted at the base of the overlying Kazhdumi Formation. In seismic line in the Sirri area, interpretation of Dariyan and Sarvak features suggest the seaward advance of the carbonate platform during periods of rising sea level. The dip angle of these reflectors within the Sarvak Formation is about 1–2 degrees (Fig. 13), whereas it is lower in the Daryian and Surmeh Formations (Fig.14).

Within the Daryian Formation, a discontinuity between the upper and lower parts is interpreted as resulting from impedance contrast between carbonate layers and the shale-dominated Bab unit in Arabian part. As illustrated in Fig. 13 these prograding clinoforms terminate with a downlap geometry into deeper carbonate layers characterized by fine-grained (mudstone) facies. Seismic interpretation of the Jurassic succession in eastern Kish and the Salman field indicates that depositional events dipped toward the south, with sediment accumulation concentrated around these areas (Fig. 14). Overall, these observations suggest the formation of intra-shelf basins during the Middle Jurassic (Bathonian to Callovian), Aptian and Cenomanian as a result of deep faults activity in the eastern part of the study area.

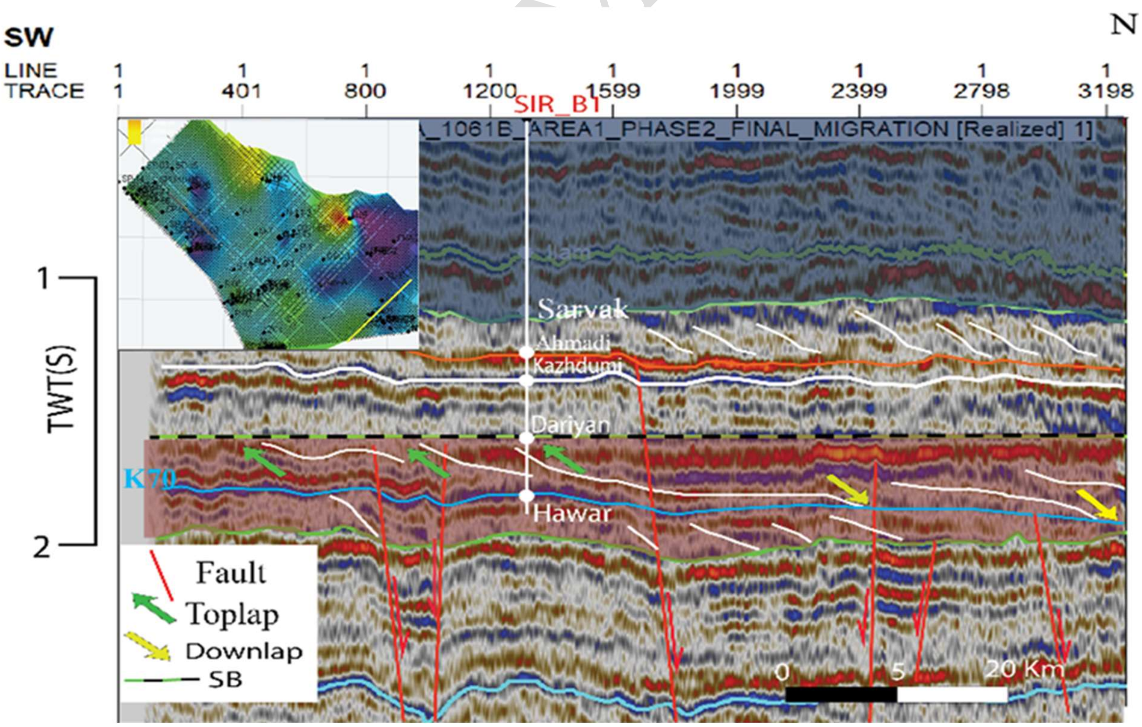

Figure 13. Seismic line shows major horizons interpretation in SIR_B1 well location, horizon flattened on Dariyan truncation reflectors is shown. 2D seismic profile with interpretation of the Intrashelf basins within the Dariyan Formation, along with the related clinoforms in the northern Sirri region. Faults relate to the Sirri fault system, Maximum flooding K70 is conicoid with Hawar Member: Base map is subsidence map

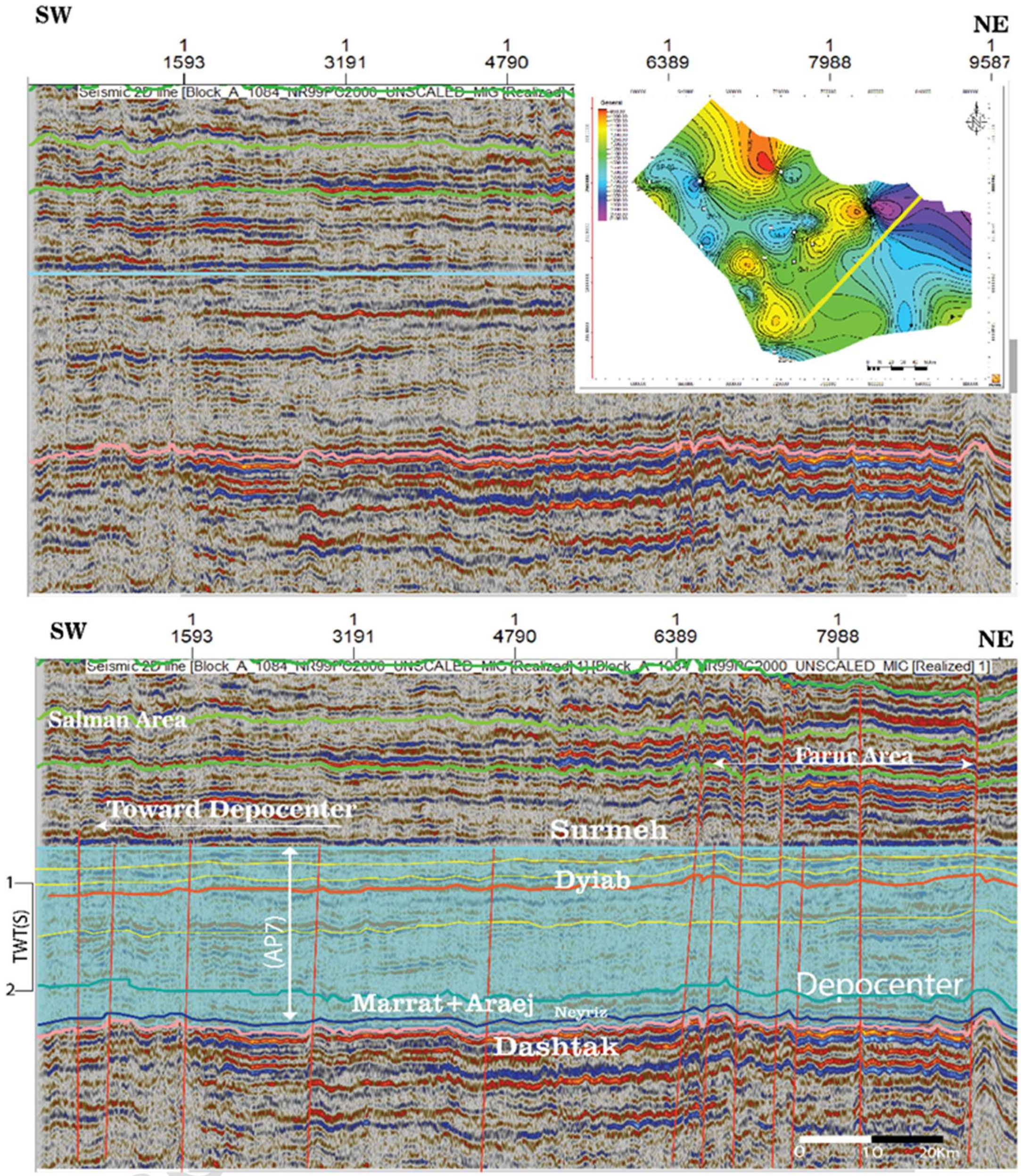

Figure 14. a) Seismic line 1084 shows major horizons interpretation on Sirri-B structure (Sirri-B1), horizon flattened on Dariyan b) 2D seismic profile with interpretation of the Intrashelf basins within the Surmeh Formation (accordance with AP7 Sharland et al. (2001), seismic line is located east of Sasan area and Farur area: Base map is subsidence map

Discussion

The integrated interpretation of basement structural maps, isopach maps, seismic profiles, and well correlations indicates that the post-Triassic evolution of the Central Persian Gulf was governed by the combined effects of deep-rooted basement fault reactivation, Hormuz Salt tectonics, and long-term eustatic sea-level fluctuations. Nevertheless, the spatial distribution of sediment thickness, facies architecture, and depocenter development demonstrates that tectonic processes exerted the primary control on accommodation generation, whereas eustatic sea-level fluctuations mainly regulated the regional extent and timing of carbonate deposition.

The interpreted basement structural map reveals a systematic alternation of uplifted and subsided basement blocks that closely corresponds to the thickness distribution of the Surmeh, Dariyan, and Sarvak Formations. Areas developed over basement highs consistently exhibit reduced stratigraphic thicknesses, whereas the thickest sedimentary successions are concentrated within structurally subsiding depocenters. This close spatial relationship suggests that repeated reactivation of inherited basement faults governed differential subsidence throughout the Jurassic and Cretaceous. The Hamoon, Bastak, Bostaneh, Razak, Hendurabi, Sirri, and Trans-Arabian fault systems collectively compartmentalized the carbonate platform into structurally controlled palaeohighs and depocenters.

The influence of basement tectonics was further modified by syn-depositional movement of the Hormuz Salt. In several parts of the study area, sediment-thickness variations coincide with salt structures, indicating that salt withdrawal enhanced localized accommodation, whereas diapiric uplift reduced depositional space above structural highs. Consequently, the present basin geometry reflects the combined effects of basement-controlled differential subsidence and salt-related deformation.

These observations are consistent with previous studies that emphasized the importance of Hormuz salt tectonics in controlling basin architecture and accommodation development (Jackson and Talbot, 1991; Hudec and Jackson, 2007; Jahani et al., 2009). Similarly, Bagherpour et al. (2021) demonstrated that reactivation of inherited basement faults associated with Neo-Tethyan tectonic evolution generated horst-and-graben geometries that exerted a first-order control on accommodation and facies distribution across the Persian Gulf, the same result is also reported by Mohammadrezaei et al. (2022) in the Bahregansar structure where deep rooted fault reduce/eroded Cenomanian to Santonian successions thickness. Comparable conclusions were reported by Daneshvar et al. (2023), who documented systematic transitions from shallow inner-ramp environments developed over structural highs to outer-ramp and basinal settings within structurally subsiding areas.

Although the development of Arabian intrashelf basins has commonly been interpreted primarily as a consequence of eustatic sea-level fluctuations (Droste, 2004; van Buchem et al., 2010; Razin et al., 2010; Bromhead et al., 2022), the results of the present study indicate that eustasy alone cannot explain the magnitude or spatial organization of sediment-thickness variations observed across the Central Persian Gulf. Instead, the strong correspondence between the faults distribution, salt structures, seismic interpretation, as well as gravity data (Eshaghzadeh et al. (2014) indicates that inherited tectonic structures established the fundamental accommodation framework.

The distribution of the Surmeh, Dariyan, and Sarvak depocenters aligns with the paleogeographic reconstructions of Wilson (2020a, d), van Buchem et al. (2010), and Bromhead et al. (2022), who interpreted the northeastern Arabian Plate as a broad passive-margin carbonate platform intersected by long-lived intrashelf basins. However, the present study further demonstrates that the geometry, persistence, and spatial distribution of these depocenters within the Iranian sector were primarily governed by repeated basement fault reactivation and were subsequently modified by progressive Hormuz salt tectonics.

Based on the integration of these observations, a conceptual tectono-sedimentary evolution model is proposed for the Central Persian Gulf (Fig. 15). Rather than representing three independent processes, the model illustrates the hierarchical interaction of the principal controls responsible for basin evolution. Basement fault reactivation established the primary structural framework and governed long-wavelength accommodation development through differential uplift and subsidence. Hormuz Salt tectonics acted as a secondary control by locally modifying basin geometry through salt redistribution, withdrawal, and diapiric growth. In contrast, eustatic sea-level fluctuations primarily influenced the timing, continuity, and regional extent of carbonate sedimentation without determining the position of the principal depocenters.

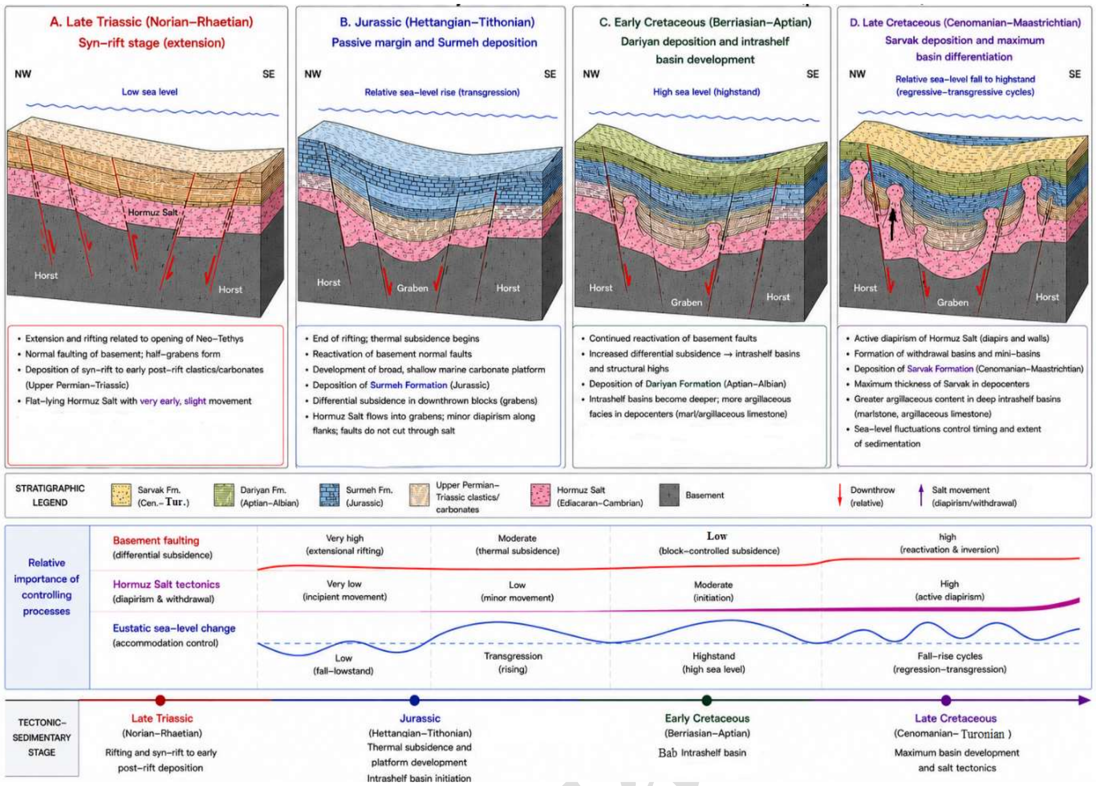

Figure 15. Schematic conceptual tectono-sedimentary evolution of the Central Persian Gulf, showing the combined influence of basement faulting, Hormuz Salt tectonics, and eustatic sea-level fluctuations on the development of intrashelf basins from the Late Triassic to the Late Cretaceous

The proposed conceptual model therefore provides a unified explanation for the observed relationships among basement morphology, sediment-thickness distribution, facies architecture, and the evolution of the Surmeh, Dariyan, and Sarvak intrashelf basins. It demonstrates that the tectono-sedimentary evolution of the Central Persian Gulf resulted from the progressive interaction of first-order basement faulting, second-order Hormuz Salt tectonics, and third-order eustatic sea-level fluctuations, which together controlled accommodation development and the long-term evolution of the basin from the Late Triassic to the Late Cretaceous (Fig. 15).

Conclusion

Employing the integrated approach which included well data, backstripping method, subsidence analysis, and 3D mapping modeling, the areas with the highest subsidence and uplift in the central Persian Gulf were identified. Interpretation of seismic data revealed structural phenomena and intrashelf basins of significant importance for hydrocarbon reservoirs. The validity of these results was confirmed through seismic sequence stratigraphic analysis a well data with clinoforms patterns in intrashelf basins of the Surmeh, Dariyan, and Sarvak Formations.

Subsidence exhibited high rates during two distinct periods: The Middle Permian and the Middle Jurassic. Reactivation of inherited structures was observed through one-dimensional backstripping analysis during four-time intervals: Triassic-Jurassic, Early Jurassic-Early Cretaceous, Mid-Cretaceous (Turonian), and Oligo-Miocene.

Deep-rooted faults including Razak (RZF), Bastak (BKF), Bostaneh (BSF), Hendurabi (HDF), Hamoon (HF), and Sirri fault system were shown to be first-order controls on basin architecture and sedimentation. Their activity created localized accommodation zones, promoting carbonate deposition.

In this study, the Hamoon-Balal and Sirri intrashelf basins were introduced as well as identified, along with other intrashelf basins situated around salt structures and basement faults. This research has precisely determined the location of these basins in the eastern Persian Gulf for the first time, showing significant conformity with findings from the UAE and Qatar regions (Davies et al., 2002; Wilson, 2020d; Bromhead et al., 2022).

Acknowledgements:

This paper forms part of the first author's Ph.D. dissertation at Shahid Beheshti University. The Iranian Offshore Oil Company (IOOC) and Shahid Beheshti University are gratefully acknowledged for providing data and analytical support. The authors also wish to thank the two anonymous reviewers for their constructive comments, which significantly improved the manuscript.

Conflicts of interest

The authors declare that they have no known competing financial interests or personal relationships that could have appeared to influence the work reported in this paper.

Author Contributions

Jaber Shoghi: Methodology, Software, Formal analysis, Investigation, Data curation, Visualization, Writing – original draft.

Seyed Ahmad Alavi: Conceptualization, Supervision, Validation, Writing – review & editing. Ehsan

Dehyadegari: Data curation, Methodology, Supervision, Validation, Writing – review & editing.

Iraj Abdollahie Fard: Geological interpretation, Resources, Validation, Writing – review & editing.

References

Abdollahie Fard, I., Sherkati, Sh., McClay, K., Haq, B. U., 2019. Tectonosedimentary evolution of the Iranian Zagros in a global context and its impact on petroleum habitat. In Developments in structural geology and tectonics (Vol. 3, pp. 17–28). Elsevier.

Agard, P., Omrani, J., Jolivet, L., Mouthereau, F., 2005. Convergence history across Zagros (Iran): constraints from collisional and earlier deformation. International Journal of Earth Sciences 94, 401–419.

Alavi, M., 2004. Regional stratigraphy of the Zagros fold-thrust belt of Iran and its pro-foreland evolution. Am J Sci 304:1–20

Al-Husseini, M., 2000. Origin of the Arabian Plate structures: Amar collision and Najd rift. GeoArabia, 5(4), 527–542. https://doi.org/10.2113/geoarabia0504527.

Allen, P. A., Allen, J. R., 2013. Basin analysis: Principles and application to petroleum play assessment. John Wiley & Sons.

Bahroudi, A., Talbot C. J., 2003. The configuration of the basement beneath the Zagros basin. Journ Petrol Geol 26:257–282.

Berberian, M., King, G.C.P., 1981. Towards a paleogeography and tectonic evolution of Iran. Canadian Journal of Earth Sciences 18, 210e265.

Bromhead, A. D., Van Buchem, F. S. P., Simmons, M. D., Davies, R. B., 2022. Sequence stratigraphy, palaeogeography and petroleum plays of the Cenomanian–Turonian succession of the Arabian Plate: An updated synthesis. Journal of Petroleum Geology, 45(2), 119-161.

Bordenave, M. L., 2014. Petroleum systems and distribution of the oil and gas fields in the Iranian part

of the Tethyan region.
Cohen, K. M., Harper, D. A. T., Gibbard, P. L., Car, N., 2023. ICS International Chronostratigraphic Chart 2023/09.
Davies, R. B., Casey, D. M., Horbury, A. D., Sharland, P. R., Simmons, M. D., 2002. Early to mid-Cretaceous mixed carbonate-clastic shelfal systems: examples, issues and models from the Arabian Plate. GeoArabia, 7(3), 541-598.
Dyer, R. C., Husseini, M. I., 1991. The tectonic evolution of the Arabian Plate and the Gulf of Aden. In: The Arabian Plate and Its Hydrocarbon Potential (eds. M. I. Husseini), Journal of Petroleum Geology, Special Publication 2, pp. 265–291.
Eshaghzadeh, A., Parto, M., Hekmat, Z. M., 2014. 3-D gravity modeling of basement reliefs an offshore case study in the Persian Gulf, Iran. International Journal of Basic and Applied Sciences, 3(3), 291.
Faqira, M., Rademakers, M., Afifi, A. M., 2009. New insights into the Hercynian Orogeny, and their implications for the Paleozoic Hydrocarbon System in the Arabian Plate. GeoArabia, 14(3), 199-228.
Goldhammer, R. K., 1997. Compaction and decompaction algorithms for sedimentary carbonates. Journal of Sedimentary Research, 67(1), 26-35.
Haq, B., Hardenbol, J., Vail, P., 1987. Chronology of fluctuating sea levels since the Triassic. Science, 235(4793), 1156–1167. https://doi. org/10.1126/science.235.4793.1156.
Haq, B., Al-Qahtani, A. M., 2005. Phanerozoic cycles of sea-level change on the Arabian Platform. GeoArabia 10(2), 127–160. https://doi.org/10.2113/geoarabia1002127.
Konert, G., Al-Afifi, A, M., Al-Hajri, S. A., Droste, H. J., 2001. Paleozoic stratigraphy and hydrocarbon habitat of the Arabian Plate. GeoArabia 6(3):407–442
Jabir, M. A., Ali, M.Y., Ismaiel, M., Watts, A. B., 2023. Subsidence and uplift history of the UAE and the western flank of the UAE-Oman mountain range. Tectonics, 42, e2023TC007998. https://doi.org/10.1029/2023TC007998
Jahani, S., Callot, J. P., Letouzey, J., De Lamotte, D. F., 2009. The eastern termination of the Zagros Fold-and-Thrust Belt, Iran: structures, evolution, and relationships between salt plugs, folding, and faulting. Tectonics 28:22.
Jahani, S., Hassanpour, J., Mohammadi-Firouz, S., Letouzey, J., De Lamotte, D. F., Alavi, S. A., Soleimany, B., 2017. Salt tectonics and tear faulting in the central part of the Zagros Fold-Thrust Belt, Iran. Marine and Petroleum Geology, 86, 426-446.
Mehrabi, H., Rahimpour-Bonab, H., Hajikazemi, E., Jamalian, A., 2015. Controls on depositional facies in Upper Cretaceous carbonate reservoirs in the Zagros area and the Persian Gulf, Iran. Facies, 61, 1-24.
Mohammadrezaei, H., Alavi, S. A., Ghanadian, M., Ghassemi, M. R., 2022. The effects of wrench-dominated basement-involved faults on folding of overlying strata in the Bahregansar anticline, western Persian Gulf, Iran. Comptes Rendus. Géoscience, 354(G1), 105-118.
Motamedi, H., Pourkermani, M., 2009. Structural Style Variation in the Central Fars Area Southern Zagros Folded Belt, Iran. In Shiraz 2009-1st EAGE International Petroleum Conference and Exhibition (pp. cp-125). European Association of Geoscientists & Engineers.
Murris, R. J., 1980. Middle East: stratigraphic evolution and oil habitat. AAPG Bulletin, 64(5), 597-618.
Orang, K., Motamedi, H., Azadikhah, A., & Royatvand, M., 2018. Structural framework and tectono-stratigraphic evolution of the eastern Persian Gulf, offshore Iran. Marine and Petroleum Geology, 91, 89-107.
Schmoker, J. W., Halley, R. B., 1982. Carbonate porosity versus depth: a predictable relation for south Florida. AAPG Bull 66:2561–2570.
Sclater, J.G., Christie, P.A.F., 1980. Continental stretching: an explanation of the post-Mid-Cretaceous subsidence of the Central North Sea basin. Journal of Geophysical Research, 85, 3711–3739. https://doi.org/10.1029/jb085ib07p03711.
Sepehr, M., Cosgrove, J. W., 2007. The role of major fault zones in controlling the geometry and spatial organization of structures in the Zagros Fold-Thrust Belt. In: Deformation of the Continental Crust: The Legacy of Mike Coward (Ed. by Ries, A.C. Butler, R.W.H., and Graham, R.H.). Special Publications, Geological Society, London, Vol.272: p.419-436.
Sharland, P.R., Archer, R., Casey, D.M., Davies, R.B., Hall, S., Heward, A., Horbury, A., Simmons,

M.D., 2001. Arabian Plate Sequence Stratigraphy. GeoArabia Special Publication No.2, 371p. Gulf Petrolink, Bahrain.
Sherkati, S., Letouzey, J., Frizon de Lamotte, D., 2006. Central Zagros fold-thrust belt (Iran): New insights from seismic data, field observation, and sandbox modeling. Tectonics, 25(4).
Shoghi, J., Alavi, S.A., Abdollahie Fard, I., Davies, R. B., Dehyadegari, E., 2025. New insight into subsidence and uplift history of the Central Persian Gulf, offshore Iran. Research Square Preprint. https://doi.org/10.21203/rs.3.rs-7795420/v1.
Simmons, M.D., Bidgood, M.D., Davies, R.B., Droste, H., Levell, B., Razin, P., van Buchem, F.S.P., 2025. Intra-Turonian stratigraphic reorganization on the Arabian Plate. Geological Society, London, Special Publications 545(1), SP545-2023.
Simmons, M.D., Sharland, P.R., Casey, D.M., Davies, R.B., Sutcliffe, O.E., 2007. Arabian Plate sequence stratigraphy: potential implications for global chronostratigraphy. GeoArabia 12(4), 101–130.
Stewart, S. A., 2016. Structural geology of the Rub' Al-Khali Basin, Saudi Arabia, Tectonics, 35, 2417–2438, doi:10.1002/2016TC004212.
Vahrenkamp, V.C., Van Laer, P., Franco, B., Celentano, M.A., Grelaud, C., Razin, P., 2015. Late Jurassic to Cretaceous source rock-prone intrashelf basins of the Eastern Arabian Plate: interplay between tectonism, global anoxic events and carbonate platform dynamics. In: International Petroleum Technology Conference, p. D021S002R003.
Vail, P. R., 1987. Seismic stratigraphy interpretation using sequence stratigraphy: Part 1: Seismic stratigraphy interpretation procedure.
Van Buchem, F.S.P., Al-Husseini, M.I., Maurer, F., Droste, H.J., Yose, L.A., 2010. Sequence-stratigraphic synthesis of the Barremian – Aptian of the eastern Arabian Plate and implications for the petroleum habitat. In F.S.P. van Buchem, M.I. Al-Husseini, F. Maurer and H.J. Droste (Eds.), Barremian – Aptian stratigraphy and hydrocarbon habitat of the Eastern Arabian Plate. GeoArabia Special Publication 4, Gulf PetroLink, Bahrain, v. 1, p. 9-48.
Van der Meer, D., van Saparoea, A., Van Hinsbergen, D., Van de Weg, R., Godderis, Y., Le Hir, G., Donnadieu, Y., 2017. Reconstructing first-order changes in sea level during the Phanerozoic and Neoproterozoic using strontium isotopes. Gondwana Research, 44, 22–34. https://doi.org/10.1016/j.gr.2016.11.002
Wilson, A.O., 2020a. Structural development of the Arabian Intrashelf Basin region. Geological Society, London, Memoirs, 53,
https://doi.org/10.1144/M53.2
Wilson, A.O., 2020d. Introduction to the Jurassic Arabian Intrashelf Basin. Geological Society, London, Memoirs, 53, https://doi.
org/10.1144/M53.1.